JOM, Vol. 69, No. 10, 2017
DOI: 10.1007/s11837-017-2337-3

Cleaner Production of Ti Powder by a Two-Stage Aluminothermic Reduction Process

KUN ZHAO,[1,3] YAOWU WANG,[1] and NAIXIANG FENG[1,2]

1.—School of Metallurgy, Northeastern University, Shenyang 110819, People's Republic of China. 2.—e-mail: fengnaixiang@163.com. 3.—e-mail: zkngwt@126.com

A two-stage aluminothermic reduction process for preparing Ti powder under vacuum conditions using Na_2TiF_6 was investigated. An Al-Ti master alloy and a clean cryolite were simultaneously obtained as co-products. The first-stage reduction was an exothermic process that occurred at approximately 660°C. The Al and O contents of the Ti powder product were 0.18 wt.% and 0.35 wt.%, respectively, with an average particle size < 74 μm. Ti(IV), Ti(III), and metallic Ti were present in the Ti-containing cryolite produced by the first-stage reduction, at a total content of approximately 3.13 wt.%. After second-stage reduction, the Ti elemental contents of the clean cryolite were reduced to 0.002 wt.%. The Al-Ti master alloy obtained by second-stage reduction was composed of Al and $TiAl_3$. The mechanisms involved in these reduction processes were also examined.

INTRODUCTION

Titanium is a noteworthy metal for many applications because of its unique combination of physical and chemical properties, including its low density, high specific strength, fatigue resistance, corrosion resistance, and biocompatibility.[1] Increased interest in various structural applications has motivated recent investigations into the development of titanium alloys, which are regarded as alternative materials for steel and Al as a result of their high oxidation resistance, favorable creep behavior, and processability.[2] Therefore, metallic titanium and its alloys have received extensive attention in certain advanced technologies, including aerospace, navigation equipment, automobiles, and biomedical artificial organs.[3]

Traditional wrought methods for producing titanium components are characterized by low yields and high costs, thus, limiting the industrial applications of titanium.[4] Powder metallurgy (PM), including near-net-shape technologies, has been suggested as a low-cost manufacturing alternative to traditional wrought methods.[5] Titanium and its alloy powders, the most common materials used in PM, play an important role in the field of titanium processing. Currently, low-cost titanium powder is typically prepared by a hydrogenation–dehydrogenation (HDH) process using titanium sponge as the starting material.[6] The titanium sponge is hydrogenated to form brittle TiH_2 pieces, which are subsequently crushed into a fine powder and dehydrogenated under vacuum at temperatures above 300°C to obtain titanium powder. Nevertheless, the conventional metallurgical route for producing titanium sponge, the Kroll process, is disadvantageous with respect to labor and energy requirements, making the production of titanium sponge a costly process.[7]

To date, the existing approaches for producing titanium have focused primarily on two methods: electrochemical reduction and metallothermic reduction. Because of its short process flow and low pollution production, electro-deoxidation is a key new research direction in the field of titanium metallurgy, and it yields titanium powder. A variety of titanium-containing compounds (TiO_2, K_2TiF_6, K_2TiO_3, $CaTiO_3$, TiC_xO_y) can be used as precursors during these electrolysis experiments.[8–12] Nevertheless, electro-deoxidation processes feature some problems such as low efficiency and difficult post-treatment requirements. Although it is considered a potential replacement for the Kroll process, electrochemical reduction needs further development before it can be used on a commercial scale. Even though the Kroll process is a typical metallothermic reduction method,[13] aluminothermic reduction has also been reported for the recovery

(Published online April 7, 2017)

of titanium from TiO_2 and K_2TiF_6.[14–18] Nonetheless, these methods are less than ideal owing to the low product quality (Ti content ≤97.01 wt.%) and high costs associated with this process. Therefore, developing a shorter, simpler, and less costly process for preparing pure titanium is significantly important in the field of metallurgy. Preparation of high-quality Ti powder at low cost has also become a clear technological challenge for the titanium manufacturing industry.

Vacuum metallurgy is considered to be a feasible means of separating metals and slag via evaporation in an ecofriendly manner. In this work, we designed an ecofriendly two-stage vacuum aluminothermic reduction process for preparing Ti powder from Na_2TiF_6. Clean cryolite was also obtained as a co-product of this new process. This report examines this process in detail, and it presents experimental evidences in favor of this new approach. The main reaction mechanism is discussed, and a concept for a continuous cyclic route is proposed.

EXPERIMENTAL

Na_2TiF_6 (≥98%, particle size < 74 μm) was used as the titanium source, and Al powder (≥99.9%, particle size < 74 μm) was used as the reducing agent. The oxygen contents of Na_2TiF_6 and Al powders were detected by an oxygen–nitrogen determinator prior to the experiment, and they were 0.34 wt.% and 0.09 wt.% respectively. Na_2TiF_6 was mixed with Al powder at a Na_2TiF_6-to-Al molar ratio of 3:4. The mixture was ball-milled for 12 h, and then it was compacted into blocks 25 mm in diameter and 30 mm in height under a compacting pressure of 40 MPa using a double-action molding pressing testing machine. Afterward, a molybdenum crucible filled with block masses was placed at the bottom of a vacuum furnace. Argon gas was flushed into the furnace to saturation to ensure that the reduction process was carried out under a pure argon atmosphere. Then, water was poured into the jacket as a coolant, and the apparatus was heated to 1050°C at a rate of 10°C × min^{-1}. After completion of the reduction reaction, the vacuum distillation process was initiated at a pressure < 0.1 Pa. Over a period of time, the sample was cooled to room temperature under vacuum. The product was removed from the crucible, and the crystallized product was collected from the condenser. Lastly, the crystallized product was mixed with Al powder with a mass ratio of 10:3 and calcined for 2 h under argon at 1050°C to complete the second-stage reduction process.

Thermal gravimetric analysis of the first-stage reduction process was carried out using thermogravimetry–differential scanning calorimetry (TG-DSC) methods. The crystal structures of reduction products were identified by x-ray diffraction (XRD) measurements with a Cu-Kα characteristic ray and energy-dispersive spectrometry (EDS). The morphologies of the reduction products were observed using scanning electron microscopy (SEM). X-ray photoelectron spectroscopy (XPS) was used to characterize the form of Ti present in the crystallized product. Inductively coupled plasma-atomic emission spectrometry (ICP-AES) was used to examine the impurities present in the final product and co-product.

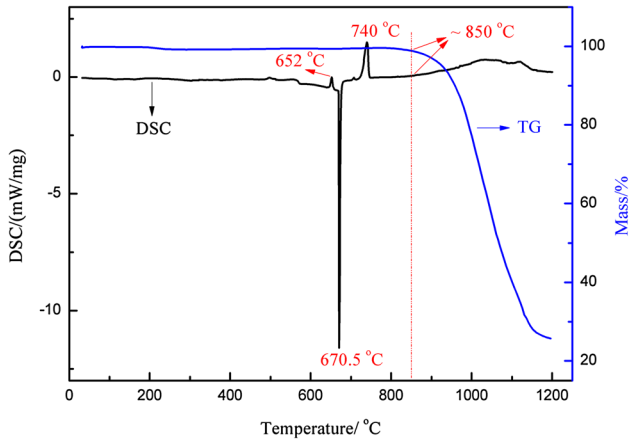

Fig. 1. TG-DSC curves of the first stage aluminothermic reduction process.

RESULTS AND DISCUSSION

TG-DSC Analysis of the Reduction Process

TG-DSC analysis was performed on the mixture of Na_2TiF_6 and Al powders to understand the conditions of the reduction reaction. This analysis was carried out under an argon atmosphere from 35°C to 1200°C at a heating rate of 10°C × min^{-1}. Figure 1 illustrates the TG-DSC spectrums. Three peaks are present in DSC spectrum, two of which denote endothermic behavior. The first endothermic signal was at approximately 650°C, which likely corresponds to the molten form of Al. A narrow and sharp exothermic peak was also present at approximately 660°C associated with a fast exothermic reaction, denoting the aluminothermic reduction of Na_2TiF_6. These two signals were detected one after another over a very short time period, suggesting that the first-stage aluminothermic reduction process occurred at the melting moment of Al. Influenced by the exothermic signal of the reduction reaction, the endothermic signal of Al molten is much less pronounced. The third signal at approximately 740°C was the endothermic melting peak of chiolite ($Na_5Al_3F_{14}$). When the temperature reached 850°C, the heat absorption of the reaction system can be observed in the DSC curve, which may be caused by the melting of cryolite. On this account, the decreased mass reflected in the TG curve was attributed to the volatile nature of cryolite.

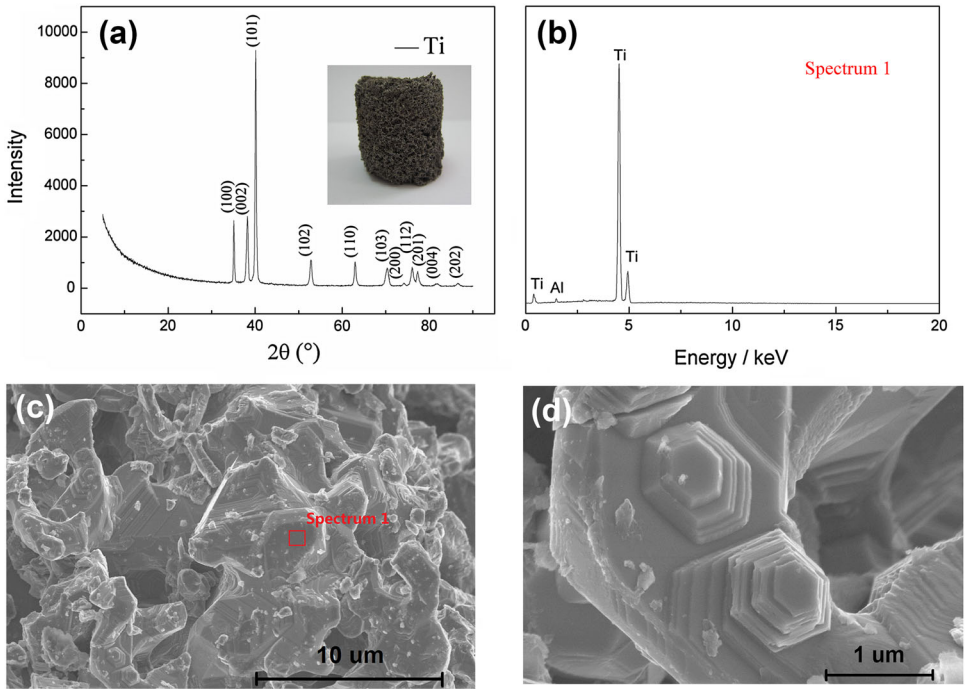

Fig. 2. XRD pattern (a) of the reduction product obtained after the first stage process, and inset of (a) shows its original form photo; EDS spectrum (b) of the reduction product (specture 1 in (c)); SEM images (c) and (d) of the reduction product at different magnifications.

Characterization of the Reduction Product and Distilled Product

Figure 2a shows the XRD pattern of the reduction product obtained after the first-stage reduction. The diffraction peaks were all indexed to a single phase of Ti (referenced to JCPDS No. 01-089-5009), meaning that the first-stage reduction process was completed in these conditions. The inset of Fig. 2a shows the original appearance of the reduction product, exhibiting a structure similar to a loose sponge. Gentle lapping allowed for titanium powders of different particle sizes to be obtained. The EDS spectrum of the reduction product is shown in Fig. 2b. It is notable that the main peaks were all associated with Ti but that a wavelet corresponding to Al also was observed. As shown in Fig. 2c, the morphology of the reduction product was a sponge-like frame structure. At increased magnification, a clear hexagonal crystal structure was observed (Fig. 2d). Taking a wider view of the total procedure of the first-stage reduction, the main impurities in the reduction product must be Al and O. For this reason, ICP-AES was used to determine the Al contents, and the O contents were determined using an oxygen–nitrogen analyzer. From these analyses, the Al and O contents of the milled reduction product (particle size <74 μm) were 0.18 wt.% and 0.35 wt.%, respectively.

The XRD pattern shown in Fig. 3a indicates that the distilled product obtained from the first-stage reduction consisted primarily of Na_3AlF_6 and $Na_5Al_3F_{14}$, but a few peaks associated with Na_3TiF_6 were also present. This demonstrates that a low valence form of titanium could be generated as an intermediate as a result of the incomplete reaction of Na_2TiF_6 and Al. Obviously, we cannot deny that a certain amount of metallic titanium may be pumped into the co-product during the vacuum distillation process. Nevertheless, lower titanium contents cannot be detected by XRD. Figure 3b shows Ti 2p photoelectron spectra for the distilled product, which reveals that Ti was presented in the forms of Ti (0), Ti(IV), and Ti(III). The inset of Fig. 3b indicates that the distilled product was a black material, in contrast to the expected color of pure cryolite (white). The titanium contents of the distilled product as surveyed by ICP-AES were approximately 3.13 wt.%, which should be the primary cause of the blackened co-product obtained after the first-stage reduction process. For convenience, we defined this black distilled product as Ti-containing cryolite.

Results of the Second-Stage Reduction Process

Taking into account the economic benefits and necessary environmental protections, it is important to be able extract the elemental Ti contained within the Ti-containing cryolite. An image of the crucible section obtained after the second-stage reduction is shown in Fig. 4a. The Ti-containing cryolite was bleached, and a metal ingot was obtained after second-stage reduction. Figure 4b shows the XRD trace of the bleached cryolite. As

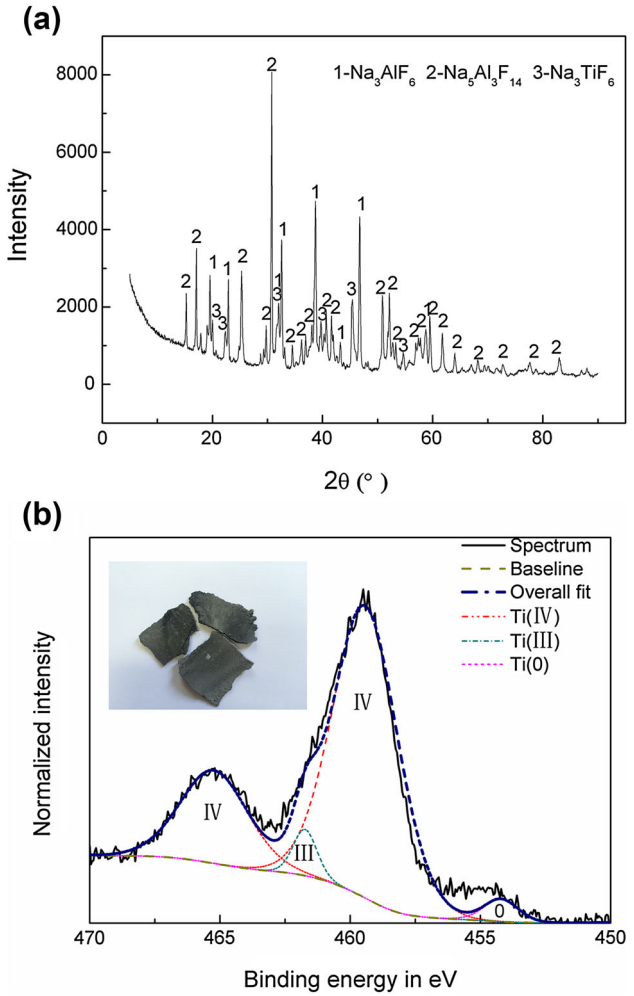

Fig. 3. XRD trace (a) of the distilled product after reduction process; XPS survey (b) of Ti 2p peaks of the distilled product and the inset of (b) displays its original form photo.

expected, all diffraction peaks could be attributed to Na_3AlF_6 and $Na_5Al_3F_{14}$. Furthermore, the Ti contents of the bleached cryolite as measured by ICP-AES were as low as 0.002 wt.%. These results indicate that the Ti formerly contained in the Ti-containing cryolite was thoroughly removed. Figure 4c shows a micrograph of the Al-Ti master alloy obtained from second-stage reduction. The result of EDS analysis demonstrates that the Ti in the Al–Ti master alloy existed in the form of $TiAl_3$, which was contained within the Al matrix. Furthermore, $TiAl_3$ was present in both granular and slender needle-like forms.

An evident boundary between the two $TiAl_3$ structures can be observed in Fig. 4c. Granular $TiAl_3$ particles were stacked densely below the boundary, while the needle-like $TiAl_3$ was sporadically distributed above the boundary. Obviously, the content of granular $TiAl_3$ was higher than that of needle-like $TiAl_3$. $TiAl_3$ is denser than Al, and the amount of $TiAl_3$ present can influence the melting point of the Al-Ti master alloy. At the beginning of the secondary reduction, $TiAl_3$ particles that settled to the bottom from the upper region, and particles generated near the bottom of the crucible, led to the increase of the melting point of the bottom alloy. For this reason, it can be deduced that the bottom alloy will solidify before the $TiAl_3$ grains grow. Nevertheless, as a result of the sufficient amount of molten aluminum present, the melting point of upper alloy is lower. This indicates that $TiAl_3$ grains generated in the upper region have sufficient time to grow until the upper alloy completely solidifies. This alloy-containing Al matrix and $TiAl_3$ intermediate phase is known as an Al-Ti master alloy.

DISCUSSION OF THE REDUCTION PRINCIPLE AND IMPROVEMENTS

K_2TiF_6-Al systems have been studied in previous reports,[19–21] which concluded that K_2TiF_6 decomposes to KF and TiF_4 (g) as follows:

$$K_2TiF_6 = 2KF + TiF_4(g) \quad (1)$$

Lee et al. examined the decomposition pressure of Na_2TiF_6, and found that the vapor pressure of Na_2TiF_6 is higher than that of K_2TiF_6.[22] Nevertheless, according to Prasad and Adamkovicova,[23,24] fluotitanate is stable at temperatures below its melting point. In the TG-DSC analysis presented in this report, there are no endothermic peaks attributed to the decomposition or melting of Na_2TiF_6. Moreover, the melting point of fluotitanate is higher than that of Al. That is to say, when the reduction reaction occurs at approximately 660°C, Na_2TiF_6 remains in a solid state. Fresh liquid aluminum is exposed at the melting moment, which promotes the reduction process. In this case, the reduction process is a solid–liquid reaction, which can be represented as follows:

$$12Na_2TiF_6 + 16Al = 12Ti + 3Na_3AlF_6 + 3Na_5Al_3F_{14} + 4AlF_3 \quad (2)$$

Combined with this analysis and the XRD and XPS evaluation of the co-product, the secondary reduction reaction likely occurs as follows:

$$3Na_2TiF_6 + 2Al = Ti + 2Na_3TiF_6 + 2AlF_3 \quad (3)$$

Although this new process marks a significant achievement, there is still room for improvement. The quality of the reduction product must meet strict requirements regarding the impurities in the pure Ti powder, including a requirement for low oxygen contents. In the present study, there is no significant change between the oxygen content of the Na_2TiF_6 feedstock and the final powder product. This means that improving the purity of Na_2TiF_6 feedstock used in this process should result in Ti powder with higher purity. The Al impurity in the

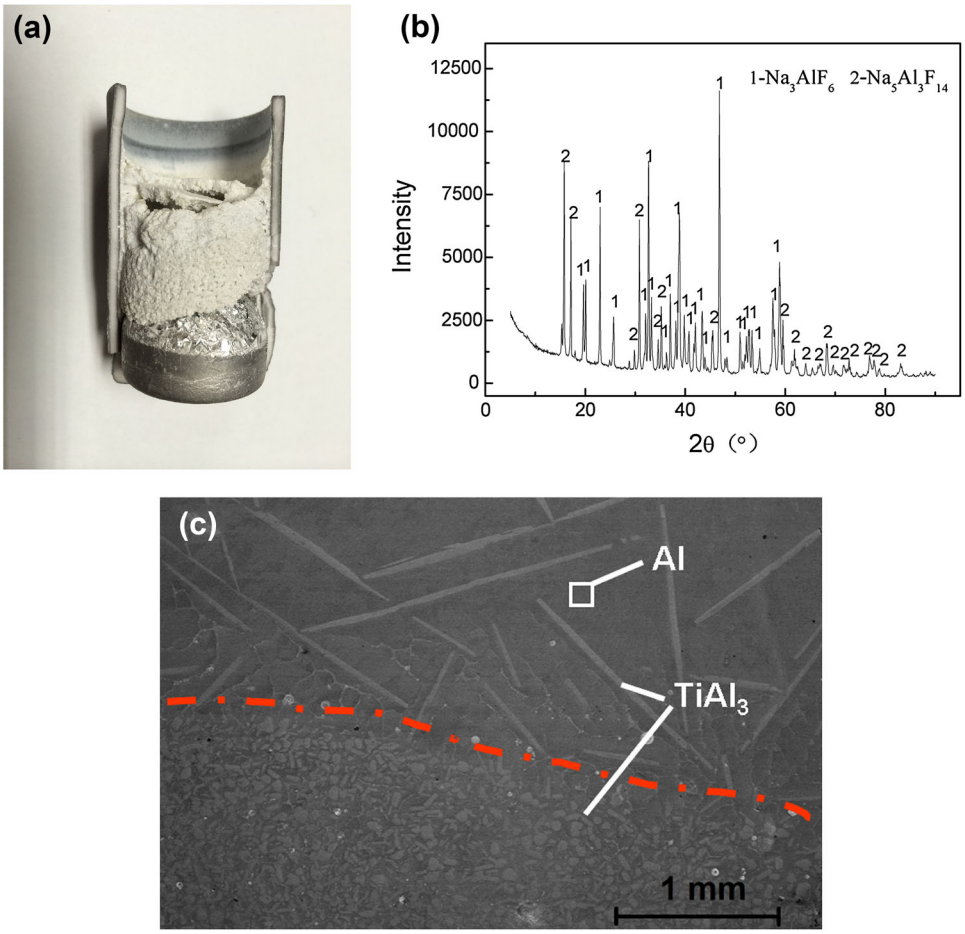

Fig. 4. Picture of the crucible section obtained after the secondary reduction (a), XRD trace of the bleached cryolite (b) and micrograph of the Al-Ti master alloy (c).

product could be diminished by reacting Na_2TiF_6 with Al in a stoichiometric ration that favors Na_2TiF_6.

SUMMARY

Metallic Ti, Al-Ti master alloy, and neat cryolite could be simultaneously obtained using the two-stage aluminothermic reduction process presented in this article. Based on thermal analysis, the first-stage aluminothermic reduction of Na_2TiF_6 was an exothermic process that proceeded quickly at approximately 660°C. The Al and O contents of the milled Ti powder (particle size <74 μm) obtained after reduction were 0.18 wt.% and 0.35 wt.%, respectively. Ti was present in the Ti-containing cryolite in the form of Ti (0), Ti(IV), and Ti(III), at total contents of approximately 3.13 wt.%. After second-stage reduction, the Ti contents of the clean cryolite decreased to approximately 0.002 wt.%. The Al-Ti master alloy obtained after second-stage reduction was composed of an Al matrix and a $TiAl_3$ intermediate phase with two structures: granular and slender needle-like structures. Almost all of the Ti from Na_2TiF_6 was extracted via this two-stage aluminothermic reduction process. With no waste products or pollution produced, this method is a simple, ecofriendly, effective, and promising path forward in the development of the titanium metallurgy industry.

ACKNOWLEDGEMENTS

This work was supported in part by the National Natural Science Foundation of China (Grant No. 51674076) and the State Key Development Program for Basic Research of China (973 Program, Grant No. 2013CB632606-1).

REFERENCES

1. Y. Zhang, *Can. Metall. Q.* 53, 440 (2014).
2. H.H. Nersisyan, H.I. Won, C.W. Won, A. Jo, and J.H. Kim, *Chem. Eng. J.* 235, 67 (2014).
3. M. Khodaei, M. Meratian, O. Savabi, and M. Razavi, *Mater. Lett.* 171, 308 (2016).
4. L. Bolzoni, E.M. Ruiz-Navas, and E. Gordo, *Mater. Sci. Eng. A* 687, 47 (2017).
5. P. Sun, Z.Z. Fang, Y. Xia, Y. Zhang, and C.S. Zhou, *Powder Technol.* 301, 331 (2016).
6. Y. Zheng, X. Yao, J. Liang, and D. Zhang, *Metall. Mater. Trans. A* 47, 1842 (2016).

7. W.J. Kroll, *Trans. Am. Electrochem. Soc.* 78, 35 (1940).
8. G.Z. Chen, D.J. Fray, and T.W. Farthing, *Nature* 407, 361 (2000).
9. D.J. Fray and G.Z. Chen, *Mater. Sci. Technol.* 20, 295 (2004).
10. K. Ono and R.O. Suzuki, *JOM* 54, 59 (2002).
11. T. Uda, T.H. Okabe, Y. Waseda, and K.T. Jacob, *Metall. Mater. Trans. B* 31, 713 (2000).
12. S.Q. Jiao and H.M. Zhu, *J. Alloys Compd.* 438, 243 (2007).
13. K. Zhao, Y.W. Wang, J.P. Peng, Y.Z. Di, K.J. Liu, and N.X. Feng, *RSC Adv.* 6, 8644 (2016).
14. D.J. Fray, *Int. Mater. Rev.* 53, 317 (2008).
15. A.D. Hartman, S.J. Gerdemann, and J.S. Hansen, *JOM* 50, 16 (1998).
16. P. Ehrlich, *Handbook of Preparative Inorganic Chemistry*, 2nd ed. (Waltham: Academic Press, 1965).
17. M. Maeda, T. Yahata, K. Mitugi, and T. Ikeda, *Mater. Trans. JIM* 34, 599 (1993).
18. T. Yahata, T. Ikeda, and M. Maeda, *Metall. Trans. B* 24, 599 (1993).
19. N. El-Mahallawy, M.A. Taha, A.E.W. Jarfors, and H. Fredriksson, *J. Alloys Compd.* 292, 221 (1999).
20. J. Fjellstedt and A.E.W. Jarfors, *Mater. Sci. Eng. A* 413, 527 (2005).
21. J.D. Donaldson, C.P. Squire, and F.E. Stokes, *J. Mater. Sci.* 13, 421 (1978).
22. M.S. Lee, B.S. Terry, and P. Grieveson, *Trans. Inst. Min. Metall. Sect. C* 103, 26 (1994).
23. K. Adamkovičová, L. Kosa, I. Nerád, I. Proks, and J. Strečko, *Thermochim. Acta* 258, 15 (1995).
24. K.V.S. Prasad, B.S. Murty, P. Pramanik, P.G. Mukunda, and M. Chakraborty, *Mater. Sci. Technol.* 12, 766 (1996).